

Native metastable prefibrillar oligomers are the most neurotoxic species among amyloid aggregates



Marco Diociaiuti ^{a,*}, Gianfranco Macchia ^b, Silvia Paradisi ^b, Claudio Frank ^c, Serena Camerini ^b, Pietro Chistolini ^a, Maria Cristina Gaudiano ^d, Tamara Corinna Petrucci ^b, Fiorella Malchiodi-Albedi ^b

^a Department of Technology and Health, Istituto Superiore di Sanità, 00161 Roma, Italy

^b Department of Cell Biology and Neuroscience, Istituto Superiore di Sanità, 00161 Roma, Italy

^c National Center for Rare Diseases, Istituto Superiore di Sanità, 00161 Roma, Italy

^d Department of Therapeutic Research and Medicine Evaluation, Istituto Superiore di Sanità, 00161 Roma, Italy

ARTICLE INFO

Article history:

Received 10 March 2014

Received in revised form 16 May 2014

Accepted 4 June 2014

Available online 14 June 2014

Keywords:

Amyloid oligomers

Neurotoxicity

Structural biophysics

Neurodegenerative diseases

ABSTRACT

Many proteins belonging to the amyloid family share the tendency to misfold and aggregate following common steps, and display similar neurotoxicity. In the aggregation pathway different kinds of species are formed, including several types of oligomers and eventually mature fibers. It is now suggested that the pathogenic aggregates are not the mature fibrils, but the intermediate, soluble oligomers. Many kinds of aggregates have been described to exist in a metastable state and in equilibrium with monomers. Up to now it is not clear whether a specific structure is at the basis of the neurotoxicity. Here we characterized, starting from the early aggregation stages, the oligomer populations formed by an amyloid protein, salmon calcitonin (sCT), chosen due to its very slow aggregation rate. To prepare different oligomer populations and characterize them by means of photoinduced cross-linking SDS-PAGE, Energy Filtered-Transmission Electron Microscopy (EF-TEM) and Circular Dichroism (CD) spectroscopy, we used Size Exclusion Chromatography (SEC), a technique that does not influence the aggregation process leaving the protein in the native state. Taking advantage of sCT low aggregation rate, we characterized the neurotoxic potential of the SEC-separated, non-crosslinked fractions in cultured primary hippocampal neurons, analyzing intracellular Ca^{2+} influx and apoptotic trend. We provide evidence that native, globular, metastable, prefibrillar oligomers (dimers, trimers and tetramers) were the toxic species and that low concentrations of these aggregates in the population was sufficient to render the sample neurotoxic. Monomers and other kind of aggregates, such as annular or linear protofibrils and mature fibers, were totally biologically inactive.

© 2014 Elsevier B.V. All rights reserved.

1. Introduction

A number of severe neurodegenerative diseases, such as Alzheimer's, Parkinson's and Creutzfeldt–Jacob's diseases, are characterized by a misfolding process of the involved proteins [1–4]. Generally, the native protein requires the destabilization of its original conformation to enter amyloid formation pathways [5]. Amyloid proteins have no similarity in their primary, secondary or tertiary structures. However, the misfolding process leads to a common typical aggregation behavior, proceeding through several steps, which include the formation of low-molecular weight oligomers (dimers, trimers, tetramers, etc.), generally named prefibrillar oligomers (PFOs), followed by annular or linear protofibrils (APFs or LPFs), before they finally assume the insoluble mature fiber (MF) conformation, characterized by the well-known β -sheet

secondary structure. Up to now, it has never been ascertained if these species represent off- or on-pathway intermediates to amyloid fibrils [6].

The debate about the culprit behind amyloid neurotoxicity is still open. For βA , the most investigated amyloid protein, during the last two decades, a multitude of molecular assemblies have been indicated as responsible species: monomers, SDS-stable dimers, aggregates of 56 kDa (βA^{*56}), βA -derived diffusible ligands, LPFs, APFs and MFs [6, 7]. A point of agreement has, however, been reached: soluble oligomers are generally considered the toxic species, while the insoluble fibrillar structure seems to be relatively non-harmful [8]. This property is characteristic not only of disease-related proteins, but it is shared by a wide family of proteins, including synthetic peptides [9], which suggests that the amyloid oligomer represents a new generic kind of molecular structure.

Many efforts have been made to clarify which is the toxic species, among the various amyloid oligomers and if there is a direct relationship between structure and cytotoxicity [10].

The results of these studies, however, have often been obtained using proteins treated under very different conditions, and using different

* Corresponding author at: Department of Technology and Health, Istituto Superiore di Sanità, viale Regina Elena 299, 00161 Roma, Italy. Tel.: +39 06 4990 2981; fax: +39 06 4990 2137.

E-mail address: marco.diociaiuti@iss.it (M. Diociaiuti).

target cells to study the cytotoxic effect. In addition, due to the propensity of amyloid proteins to spontaneously aggregate, the samples were often non-homogeneous and, more important, the structure of the aggregates was metastable, i.e. it changed during the course of the experiments [8].

Up to now, it is widely accepted that the toxicity depends on shared structural features. This is also supported by the discovery that antibodies raised against β A protofibrils were able to recognize protofibrillar species derived from other amyloidogenic, toxic proteins [11]. The most suspect species are the low-molecular weight oligomers, such as dimers, trimers, tetramers, or the first protofibrillar species, which are all spherical in shape. These nanospheres, usually named PFOs, are the precursor of chain-like and/or APF structures. Recently, Kaye et al. [12] showed that the APFs of three proteins (namely, β A42, β A40 and α -Syn) are, structurally and functionally, a distinct type of amyloid oligomer and that only PFOs were neurotoxic.

β A is the most investigated protein in the structure–toxicity relationship of amyloid oligomers, but up to now, no systematic correlation between different oligomeric species and neurotoxicity potential has been reported. This is not surprising, given the complex dynamic equilibrium displayed by β A [13,14] and the fact that the toxic species are metastable (modified by the experimental conditions). To overcome this difficulty, Bithan and Teplow developed the Photoinduced Crosslinking of Unmodified Proteins (PICUP) method and successfully applied it to the study of amyloidogenic protein assembly [15]. Ono et al. [16] recently applied in-situ chemical cross-linking to prevent β A oligomer dissociation or growth, and were able to produce pure oligomeric populations suitable to be investigated by biophysical and biological methods. They demonstrated that the toxicity of dimers, trimers and tetramers was 3-, 8- and 13-fold higher than that of monomers, respectively. To obtain this result, they were obliged to stop the fast and spontaneous β A aggregation process, by inducing the formation of covalent bonds by PICUP. However, it is unknown whether this change affected the molecular mechanisms of neurotoxicity.

Salmon calcitonin (sCT) is an amyloid protein with very slow aggregation dynamics. This feature has made sCT very appealing from a pharmacological point of view, since fast aggregation – as exhibited by calcitonins from other species – reduces the efficacy of the hormone, when used in the treatment of osteoporosis. It is also very convenient for investigating the early stages of aggregation of amyloid proteins without the necessity of crosslinking procedures, preserving in this way the native status of the amyloid assemblies.

In previous papers, we used unfractionated sCT oligomers to investigate the amyloid structure – toxicity relationship, focusing our attention on the lipid composition of the membrane of target cells [17–19]. Here, we prepared sCT fractions enriched in different sCT oligomeric species by Size Exclusion Chromatography (SEC), which has been proposed as the technique of choice for preparing β A aggregates of defined size distribution and morphology [6] and extensively studied, from a theoretical and experimental point of view, in the resolution of mixtures of protein aggregates produced in the generation of amyloid fibrils [20]. More than other methods, it does not affect the aggregation process as it is performed in an aqueous medium, allowing preserving the native configuration of the proteins [21]. Furthermore, with SEC it is possible to reduce the slow aggregation process of sCT by carrying out the experiments at low temperature (4 °C) and in the same buffer conditions of the loaded samples. The obtained fractions were then characterized by the combined application of SDS-PAGE, Energy Filtered-Transmission Electron Microscopy (EF-TEM) and Circular Dichroism (CD) spectroscopy and tested on primary neuronal hippocampal cultures, to study neurotoxicity in terms of increased apoptosis and Ca^{2+} influx [22,23].

Our results clearly show that dimers, trimers and tetramers were the neurotoxic species. Noticeably, we found that it was sufficient for the presence of few metastable dimers, trimers and tetramers, of globular shape and mainly in Random Coil (RC) configuration, to make the sample neurotoxic.

2. Materials and methods

2.1. Preparation of aggregated sCT

Lyophilized sCT (European Pharmacopoeia, EDQM, France) was stored at -18 °C before use. Unfractionated sCT 1 mM solution was prepared by dissolving the protein in 5 mM, 75 mM phosphate buffer (PB) solutions, and in 160 mM solution (PB with NaCl), pH 7.4 and incubated at room temperature for 3 h to promote the aggregation process. sCT was also diluted in deionized water immediately before use, as suggested by Wang for bovine CT, at the same concentration [24]. A solution of 0.2 mM sCT was also prepared. These solutions were loaded in the SEC columns.

2.2. Size-exclusion chromatography (SEC)

SEC was carried out on a sephadex G75 or G50 column (GE HEALTH CARE, Milano, Italy), 500 mm high \times 20 mm in diameter, maintained at 4 °C and equilibrated in distilled water or in 5 mM, 75 mM phosphate buffer (PB) solutions, and in 160 mM solution (PB plus NaCl), pH 7.4, at a flow rate of 0.13 mL/min. The G75 column was calibrated by loading a mixture of 1.0 mg ferritin, 0.5 mg albumin and 1.0 mg cytochrome C (Combithek Boehringer, Mannheim, Germany), dissolved in 0.5 ml distilled water or 5 mM solution (PB), pH 7.4 and centrifuged at $15,700 \text{ g} \times 10 \text{ min}$. For G50 column calibration, the standard proteins used were somatostatin, aprotinin and cytochrome c. Aliquots of 1 mM sCT (0.5 ml, with or without 3 h of incubation at RT) were applied onto the column and elution was monitored by absorption at 280 nm by a variable wavelength UV detector (BIO-RAD Econo UV monitor, Hercules, CA). Fractions were collected by a Gilson FC 203B at 1.4 mL/fraction and analyzed by electron microscopy and circular dichroism and used in the biological tests. The concentrations of the fractions used in the biological tests, not adjusted before treatments, were about 8 μM .

2.3. Photo-induced cross-linking of unmodified proteins (PICUP)

Samples of sCT dissolved in water or in 5 mM solution (PB), pH 7.4 and samples from the fractions separated by SEC were treated for PICUP [25]. Briefly, 18 μl of each sample (final concentration 80 μM) was cross-linked using 1 μl of 1 mM solution of RuBpy (Tris (2,2-bipyridyl) dichlororuthenium (II) hexahydrate), and 1 μl of 20 mM ammonium persulfate (SIGMA). Cross-link reaction was performed into clear, thin-walled, 0.2 ml polymerase chain reaction tubes. The tubes were placed in a dark room into borosilicate glass tubes as support and irradiated for 2 s with a 100 W white lamp. The reaction was quickly quenched by adding 20 μl of reducing tricine/SDS-PAGE sample buffer containing 5% β -MeOH and boiled for 5 min. Samples were then analyzed by tricine/SDS-PAGE.

2.4. SDS-PAGE and MALDI-TOF analysis

sCT samples were analyzed by tricine (BIO-RAD, Hercules, CA, USA)/SDS-PAGE (70 \times 80 \times 1.5 mm mini gel), using 10% Acrylamide/Bis (32:1) (ICN Biomedicals, Inc., Aurora, Ohio USA)/(Fluka, Buchs, CH) solution as separating gel, 6.5% Acrylamide/Bis solution as spacer gel and 2.5% Acrylamide/Bis solution as stacking gel. Gels were stained by silver procedure. For protein identification, bands of interest were excised from silver-stained SDS-PAGE gels, and in gel digested overnight with bovine trypsin. One μl of the supernatant of the digestion was used for MALDI-time of flight mass spectrometer (TOF MS) analysis, using α -cyano-4-hydroxycinnamic acid as matrix. All analyses were performed using a Voyager-DE STR (Applied Biosystems, Framingham, MA, USA) TOF MS operated in the delayed extraction mode. Peptides were measured in the mass range from 750 to 4000 Da; all spectra were internally calibrated and processed via the Data Explorer software.

2.5. Energy-filtered transmission electron microscopy (EFTEM)

Negative staining was obtained using a phosphotungstic acid (PTA) 2% w/v solution, brought to pH 7.3 with NaOH. To avoid salt precipitation from PTA and/or NaOH, which can be misread as actual structures, the staining solution was filtered before each preparation through polycarbonate 0.2 μm -pore filters. A droplet of solution from PICUP-untreated, SEC fractions was deposited onto 400-mesh copper grids for electron microscopy and covered with a thin amorphous carbon film (about 20 nm). When the grid was dry, a droplet of PTA was deposited and let dry. The samples were studied with a Zeiss 902 Transmission Electron Microscope, operating at 80 kV, equipped with an electron energy loss filter. In order to enhance the contrast, the microscope was used in the Electron Spectroscopy Imaging mode filtering at $\Delta E = 0$ eV [26]. Images were acquired by a digital HSC2 CCD camera, 1 k \times 1 k pixels (Proscan GmbH, Germany) and thermostatted by a Peltier cooler model WKL 230 (LAUDA GmbH, Germany). Image analysis and quantification was performed by the digital image analyzer analysis 3.0 (SIS GmbH, Germany). With this software it is possible to enhance the contrast and sharpness of the acquired images and perform morphological quantification and statistics. The dimensional measurements were done after a careful magnification calibration of the whole imaging system on the basis of reference standards.

2.6. Circular dichroism (CD) measurements

Sample of PICUP-untreated, sCT SEC fractions were analyzed by CD measurements performed on a Jasco J-715 spectropolarimeter (JASCO Corporation, Japan) in the far-UV region (260–190 nm). All spectra, mean of 4 different scans, were blank subtracted. Quartz cells of 0.1 and 0.5 cm pathlength were employed. The spectral resolution was 0.5 nm and the speed scan 50 nm/min. All CD spectra were reported as $\Delta\epsilon = [\theta]/3300$, where $[\theta]$ is equal to $(\theta \times 100) / (l \times C)$ (θ is the measured ellipticity, C is the molar amino acidic concentration and l is the pathlength in cm). CD spectra were quantitatively analyzed by a fitting procedure performed by the CDSSTR software available at the website of the Birkbeck College of the University of London [27,28]. CD spectra were acquired on protein fractions after SEC separation.

2.7. Hippocampal cell cultures

Primary hippocampal neurons were prepared from embryonic day-18 rat brain, according to the method of Brewer et al. [29], slightly modified [30]. All experimental procedures were in line with the “Ethical principles and guidelines for scientific experiments on animals” of the Swiss Academy of Medical Sciences and national laws. After dissection, the hippocampi were treated with 2.5% trypsin and dissociated. The cells were plated in 24-well plates, containing poly-L-lysine-treated glass coverslips, in Minimum Essential Medium (MEM), containing 10% heat-inactivated fetal calf serum. After 2 h, the cell culture medium was substituted with Neurobasal medium with B27 supplement (NBM/B27, Invitrogen, Italy), 700 μl per well. At day-in-vitro (DIV) 1, 5 μM arabinosylcytosine was added. Neuronal cell cultures contained less than 1% of astrocytes, as shown by glial fibrillary acidic protein staining (data not shown). Hippocampal neurons were used at 14 DIV (mature neurons).

2.8. Single cell assay for $[\text{Ca}^{2+}]_i$ recording

For evaluation of intracellular Ca^{2+} , sample from different PICUP-untreated, sCTs fractions, were given directly to the wells on the microscope stage, after 10 min recording. Optical fluorimetric recordings with Fura-2AM were used to evaluate the intracellular calcium concentration $[\text{Ca}^{2+}]_i$. Fura-2AM stock solutions were obtained by adding 50 μg of Fura-2AM to 50 μl of 75% DMSO plus 25% pluronic acid. Cells were bathed for 60 min at room temperature with 5 μl of stock solution

diluted in 1 ml of NBM/B27, for a final Fura concentration of 5 μM . This solution was then removed and replaced with extracellular solution and the dishes were quickly placed on the microscope stage. To measure fluorescence changes, a computerized analysis system was used (ImageM; Hamamatsu Photonics, Hamamatsu, Japan). In each experiment, the ratio between the values of light intensity at 340 and 380 nm stimulation (F340/380) was recorded every 6 s [31].

2.9. Apoptosis

For apoptosis detection and immunolabeling, 300 μl of cell culture medium from each coverslip-containing well was removed and kept in the incubator (conditioned medium). The hippocampal neurons were treated with different PICUP-untreated, sCTs fractions for 20 min. The cell culture medium was then removed and substituted with the conditioned medium. After 24 h, the cells were fixed in 4% paraformaldehyde in phosphate buffered-saline (PBS), 12 M in sucrose, pH 7.4, rinsed in PBS, stained with Hoechst 33258 and observed at a Nikon fluorescence microscope. Non-apoptotic cells exhibit a diffuse nuclear fluorescence, while apoptotic nuclei appear fragmented or highly condensed. Counts of normal and apoptotic cells were done on randomly chosen microscopic fields for a total of at least 200 cells for each coverslip. Two coverslips were scored for each condition. The values obtained for each coverslip were averaged to produce a single mean value for each experiment.

2.10. Statistical analysis

Apoptosis data analysis was performed by the PRISM software package. In particular, one-way ANOVA test and Dunnett post-test of the all groups against the control group were performed with a level of confidence of 95%.

3. Results and discussion

3.1. Sample preparation

SEC columns were used to obtain samples enriched with aggregated sCT species, spontaneously formed in the loaded unfractionated samples. We used a G75 column, equilibrated and calibrated at the same ionic strengths of the loaded samples, with the aim to separate the different aggregates in a wide-size range and not to accurately determine their molecular weights. To better investigate the molecular weights of the small-size aggregates, a G50 column, accurately calibrated, was used.

Fig. 1A, B and C show the SEC profiles of sCT samples incubated in buffered solutions with decreasing salt concentrations (160 mM, 75 mM and 5 mM) and Fig. 1D shows the SEC profile of an sCT sample quickly dissolved in water, without incubation. Based on the characterization described below, performed by EF-TEM and CD experiments, four kinds of peaks can be identified and labeled: the PFO-peak, in the lowest size range (less than V_c) (Fig. 1A, B, C); the APF and LPF peaks, in the intermediate size range (around V_c) (Fig. 1C, D); the MF peak, in the highest size range (Fig. 1A).

Fig. 1 shows that the PFO peak width is directly correlated to the ionic strength of the solution. There are no peaks of APFs or LPFs in panels A and B, since the high saline concentrations induce the formation of a unique, broad peak. This confirms that, as already proposed [6], the protein aggregation is triggered by salt concentration. A clear tendency to form aggregates can be observed at high saline concentration (160 mM), where an important MF peak, located at high exclusion size, appeared (Fig. 1A). Interestingly, this peak is located at volumes $<V_0$. This strange phenomenon can be explained on the basis of a recent paper where an equilibrium partition model for SEC is presented. Briefly, in this model the amyloid aggregate morphology plays a crucial role

in determining the elution volume, modifying the volume expected after a standard column calibration [20].

In the intermediate saline condition (75 mM), only a small MF peak was observed, always located at volume $<V_0$, together with two other small peaks in the central area (Fig. 1B). The lower saline concentration reduces both the protein aggregation and the peak widths, allowing the visualization of fibril peaks.

In the lowest saline condition (5 mM), the MF peak definitely disappeared and an intense and narrow LPF peak appeared on the left side of the main PFO peak (Fig. 1C). In this saline condition, we are in the early stages of fibril aggregation and the peak width was small enough to separate the two species.

In pure distilled water (Fig. 1D), we only observed a peak located at about 10,000 Da of width comparable to that obtained in the lowest saline condition.

Peaks on the right of the main PFO peak were never observed, probably because of the low resolution and size-cut of the G75 column and the low effectiveness of the G75 column in this range. Moreover, the equilibrium partition model proposed by Hall and Huang [20] suggests that, in the case of amyloid aggregates separated by SEC, the actual molecular weights are apparent only if determined after the standard calibration. This can explain why MFs can elute faster than the void volume or trimers and tetramers together with dimers and monomers or APFs close to V_c .

Finally, we observed that all species formed under the different saline conditions were present at the same time. On the basis of this consideration, we speculate that all species of the sCT aggregates were final off-pathway products, independently derived from monomeric sCT under the different conditions.

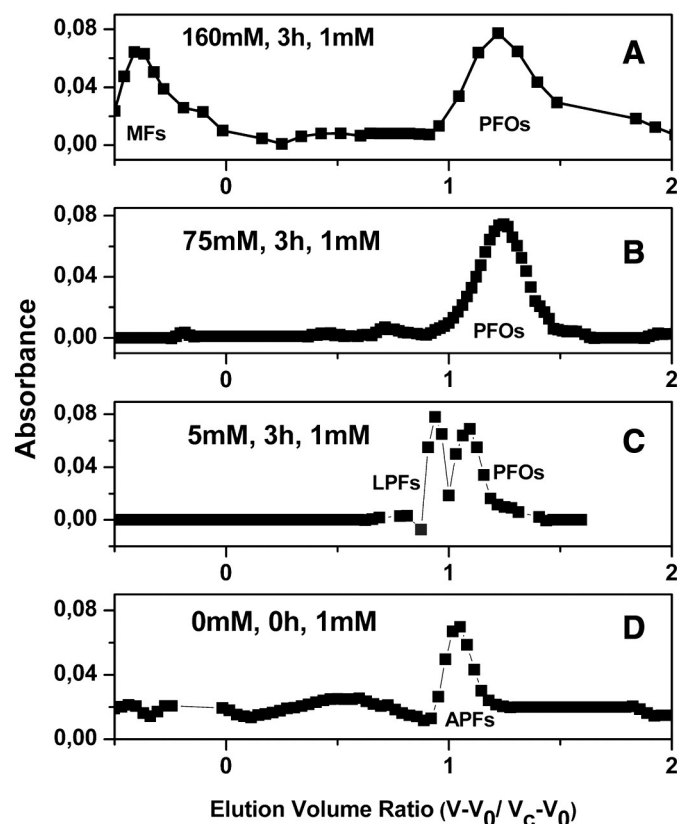


Fig. 1. The G75 column, suitable to investigate a wide molecular size range, was used. On the basis of the results of EF-TEM characterization (see below), the peaks occurred in the small size range and in all conditions and can be attributed to PFOs. Structures referable to APFs and LPFs could also be identified. High ionic strength (A) favors fiber formation, as indicated by the MFs peak. V_0 and V_c were the void and cytochrome-C elution volumes, respectively.

3.2. Sample characterization

To study aggregate size, morphology and folding, fractions representative of the detectable peaks were investigated. EF-TEM and CD spectroscopy were applied to PICUP-untreated fractions while PICUP was performed before the denaturing SDS-PAGE experiments. PICUP is a cross-linking method that i) requires short exposure of proteins to non-destructive visible light, ii) does not need modification of the native sequence, and iii) is efficient within wide pH and temperature ranges, including physiologic ones.

3.2.1. The PFO-peak

The results reported in Fig. 1 show the existence, at all the studied ionic strengths, of a main peak located in the lowest size-range ($<V_c$). This peak could be attributed, on the basis of the evaluation of the molecular weights obtained by SEC and SDS-PAGE, to a mixed population of PFOs.

All the bands were enzymatically digested by trypsin and analyzed by MALDI-MS. All bands contained only sCT (data not shown). PICUP followed by SDS-PAGE clearly shows the occurrence of monomers, dimers and an unresolved signal corresponding to trimers and tetramers (Fig. 2A, lane 1). This observation demonstrates that by the use of G75 columns, a separation of pure oligomer populations could not be obtained and that various species were simultaneously present in the sample, giving rise to the observed broad peak, located around 6800 Da. SDS-PAGE indicates that only the crosslinking (lane 1) enables dimer, trimer and tetramer visualization. When uncrosslinked, monomers and few dimers were present in the same sample (lane 2) as well as in the crosslinked, unfractionated and non-incubated sCT sample in water (lane 3).

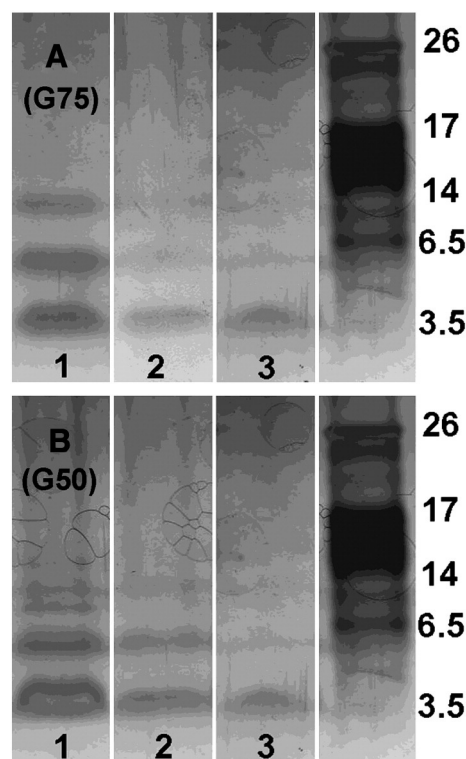


Fig. 2. Silver-stained polyacrylamide gels showing uncross-linked and photo-cross-linked sCT electrophoresis results. (A) Representative fraction of the G75 column (see Fig. 1A): cross-linked PFO peak (lane 1); uncross-linked PFO peak (lane 2); cross-linked, unfractionated and non-incubated sCT in water (lane 3). (B) Representative fraction of the G50 column: cross-linked PFO peak (lane 1); uncross-linked PFO peak (lane 2); cross-linked, unfractionated and non-incubated sCT in water (lane 3). Trimers and tetramers are well resolved in lane 1. Molecular weight standards in kDa are indicated on the right side.

We conclude that dimers, trimers and tetramers are metastable aggregates that need to be stabilized by PICUP to be identified. Conversely, monomers and few dimers were always detectable and higher molecular weight oligomers, like pentamers and so on, were totally absent.

To better investigate the occurrence of low-molecular weight aggregates, we loaded in a G50 column (5 mM PB), accurately calibrated for the molecular weight determination, an sCT sample (1 mM) incubated for 3 h in PB. In good agreement with the results obtained with the G75 column, we found the main PFO peak. However, we were able to determine that this peak is located at 6800 Da. We also observed that the LPF-peak obtained with the G75 column was located at molecular weight higher than 13,000 Da (19,000 Da) although strongly attenuated (supplementary data S1).

In Fig. 2B, we report the SDS-PAGE results regarding the crosslinked PFO peak of the G50 column (lane 1), together with the results obtained with the same sample but uncrosslinked and unfractionated (lane 2) and with a crosslinked, unfractionated and non-incubated sCT sample in water (lane 3). We note that, as in the G75 column of Fig. 2A, monomers, dimers, trimers and tetramers coexist. Considering that the same sample was loaded on G75 and G50 columns, we conclude that the highest resolution of the G50 allowed the discrimination between trimers and tetramers (Fig. 2B, lane 1), not observed in the case of G75. As in the case of the G75 column, the signal was weak for dimers and totally disappeared for trimers and tetramers when the crosslinking was not applied (Fig. 1A, lane 2). Again, this strongly supports the conclusion that PFOs, unlike monomers, were metastable aggregates that can be visualized only after PICUP that exist in the sample and may play an important biological action.

It is worth noting that few dimers were present even in the cross-linked, unfractionated sample in water (lane 3). We interpret this observation considering that, although slowly, sCT aggregation does take place even in water, in line with the amyloid nature of the protein.

We conclude that the samples obtained by SEC were composed of a mixed population of metastable dimers, trimers and tetramers, coexisting with stable monomers.

To structurally investigate the nature of the PFO peak, both EF-TEM and CD spectroscopy measurements were performed on the more representative PICUP-untreated fractions of this peak. Micrographs show the predominance of globules of 9.1 ± 3.7 nm mean diameter (Fig. 3A), while CD spectroscopy results (Fig. 3B) indicate that sCT was mainly (72%) conformed as random coil (RC). A small percentage of α and β structures were also present. Considering that, as reported by Ono's TEM direct observations [16], β A monomers and dimers are less than 2 nm in size, we interpret the images of Fig. 3A as the direct visualization of sCT metastable amyloid trimers and tetramers, evaluated to be 8- and 13-fold more toxic than the stable monomer, respectively [16]. Monomers and dimers were smaller (of about 1.5 nm) and difficult to visualize.

Finally, for what concerns the protein folding, our samples show mostly (72%) the RC configuration. This is in agreement with Ono's CD results concerning β A dimers, trimers and tetramers, which mainly showed RC CD spectra. In our case, the RC conformation is further enhanced by the coexistence of metastable PFOs with the stable RC monomers.

3.2.2. The APF-peak

We observed only a narrow peak located around V_c in the sample where sCT was dissolved in water (Fig. 1D). The nature of this peak appears completely different from the other peaks observed in the presence of salt. In fact, EF-TEM revealed the dominance of a new structure denominated APFs, of about 12 nm in diameter (Fig. 4A), previously described in literature for many other amyloid proteins. CD results showed that sCT was in RC conformation (Fig. 4B). Like in the presence of salt, we did not observe any monomer peak, probably because of the size-cut of the G75 column and the low effectiveness of the column in this range.

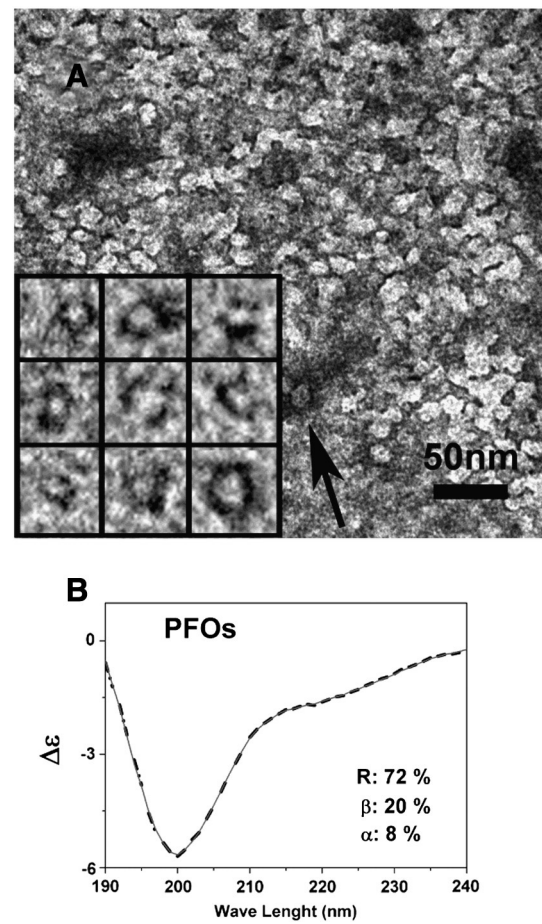


Fig. 3. (A) Representative image of PFOs obtained by negative staining and EF-TEM (arrow highlights a well-stained PFO). The sample was relative to the highest (160 mM) ionic strength. Magnifications of isolated PFOs are reported in the inset and the mean diameter measured on 84 particles was 9.1 ± 3.7 nm. (B) CD spectra (full line) together with the numerical fitting (dashed line) and the obtained structure percentages indicate that the PFOs dominant structure was RC.

APFs have been described as “amyloid-pores” due to their characteristic structure, such as those formed by β A pathogenic mutations and supposed to be at the basis of the neurotoxicity in several important diseases [32]. Several disease-related amyloid proteins form them, and it has been hypothesized that they are the common toxic species responsible for diseases [10]. However, recently Kaye clarified that APFs formed by β A40, β A42 and α -Synuclein are a structurally and functionally distinct type of oligomers and showed that, unlike PFOs, they were not able to permeabilize lipid bilayers. In neurotoxicity experiments PFOs, but not APFs, were neurotoxic. Finally, Kaye's CD results showed that the β A APFs were in the β conformation, typical of amyloid fibers [12].

Our data reported here, regarding sCT APFs, are in agreement with Kaye's morphological results, but wholly differ as for conformational results. Our data strongly indicate that sCT APFs were 73% in the RC conformation (Fig. 4B). Interestingly, it can be noted that there is a strong discrepancy between size and apparent molecular weight of this aggregate, because it is well known that the globular cytochrome C has a radius <2 nm, while we observed objects of 12 nm. This can be explained on the basis of equilibrium partition model proposed by Hall and Huang, where the morphology plays a crucial role in determining the elution volume [20].

3.2.3. The LPF-peak

In the 5 mM ionic strength G75 column, we were able to separate a narrow peak on the left portion of the main PFO peak (Fig. 1C). EF-TEM

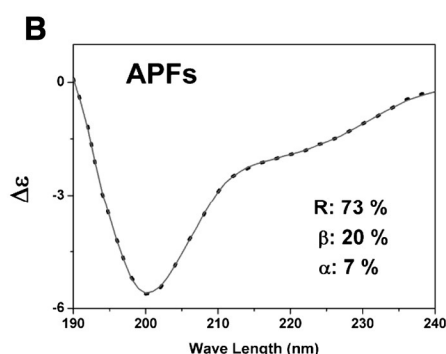
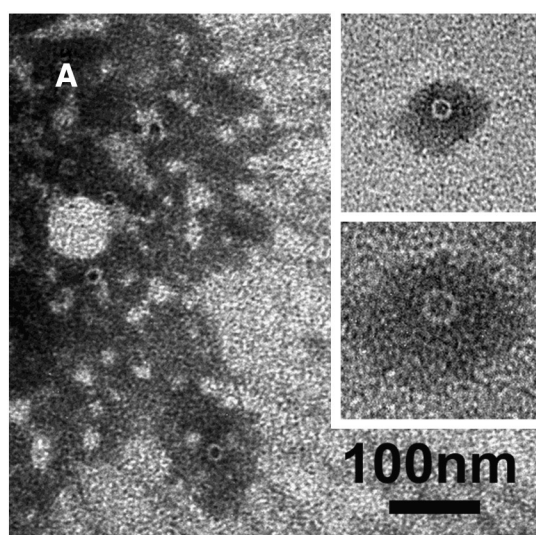


Fig. 4. (A) Representative images of APFs obtained by negative staining at EF-TEM. The sample was relative to sCT in water (Fig. 1D). Insets show higher magnifications (top inset of 91×91 nm; bottom inset of 28×28 nm) of single APFs. The mean diameter measured on 32 APFs was 12.4 ± 2.2 nm. (B) CD spectra (full line) together with the numerical fitting (dashed line) and the obtained structure percentages indicate that the APF dominant structure was RC.

images relative to this peak showed the presence of many and short (<30 nm) LPFs (Fig. 5A). Noteworthy, the initial fiber formation induced a strong protein conformation change and CD data indicated that sCT was in a mix of β (38%) and RC (59%) configuration (Fig. 5B). This sample can be considered enriched with LPFs. Even in this case, the elution volume was too close to V_c to be regarded as a reliable estimate of the actual aggregate molecular weight. As before, this is a confirmation of the partition model proposed for SEC [20].

3.2.4. The MF peak

The tendency to aggregate in high saline conditions was suggested by the existence, in Fig. 1A, of an important secondary SEC peak located at high exclusion sizes at elution volume $<V_o$. EF-TEM images revealed the presence of many typical amyloid MFs, characterized by length up to 1000 nm (Fig. 6A) and by the dominance of the well-known β – sheet conformation (82%) (Fig. 6B). As observed before, the unusual peak location can be explained on the basis that the equilibrium partition model developed for amyloid aggregates, where the fiber morphology alters the elution volumes expected after a standards column calibration [20].

In the intermediate saline condition (75 mM ionic strength, Fig. 1B), the MF peak was strongly attenuated and, given the very low protein concentration, CD results were difficult to interpret. However, a small, non-random signal (α and β structures) was detected (data not shown).

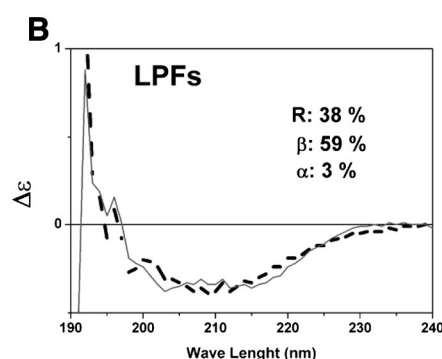
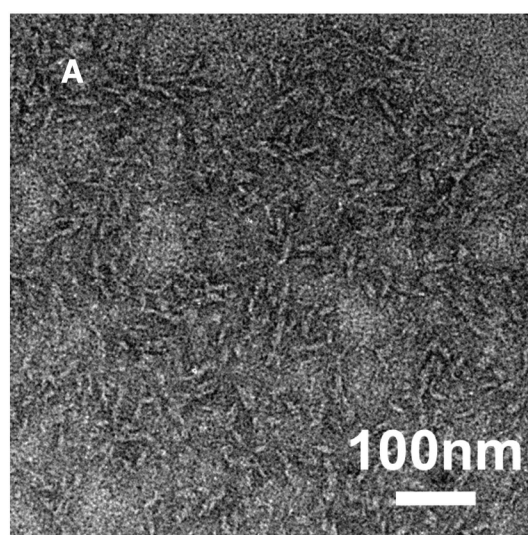


Fig. 5. (A) Representative image of very small LPFs obtained by negative staining and EF-TEM. The sample was relative to the lowest (5 mM) ionic strength. The LPFs mean length, measured on 77 particles, was 26.8 ± 8.3 nm. (B) CD spectrum (full line), together with the numerical fitting (dashed line) and the obtained structure percentages, indicates that a mixture of β and RC structures was present.

3.3. Biological effects

To investigate whether the molecular mechanism at the basis of the biological damage was related to neuron membrane permeabilization due to the formation of amyloid-channels, in our previous paper we analyzed the increase in Ca^{2+} -influx and the neurotoxic effect induced in mature primary neurons by unfractionated samples of sCT at a final concentration of 80 μM . Unfractionated samples were obtained after a preincubation in 5 mM solution (PB) at room temperature for 3 h at an sCT concentration of 1 mM [19].

Here we performed the same biological experiments to test sCT-fractionated samples obtained by SEC. We did not apply any crosslinking procedure before the biological tests and PICUP was used only to stabilize the sample before denaturing SDS-PAGE experiments. Fractions were collected without adjustment at a concentration of about 8 μM , that is 1/10 of the final concentration of the unfractionated samples used in our previous experiments.

Ca^{2+} influx experiments were performed with the SEC fractions characterized as before and results are reported in Fig. 7. We found that only populations enriched with native and metastable PFOs were able to induce a strong and immediate Ca^{2+} -influx in mature hippocampal neurons. Noteworthy, this effect was of the same order of magnitude as that observed in our previous paper, obtained with unfractionated samples, which were 10 times more concentrated [19].

It is important to note that Ca^{2+} -influx was observed only in samples rich in metastable dimers, trimers and tetramers, for both low and high saline conditions (Fig. 1A, C) and that in all other cases, no effects were

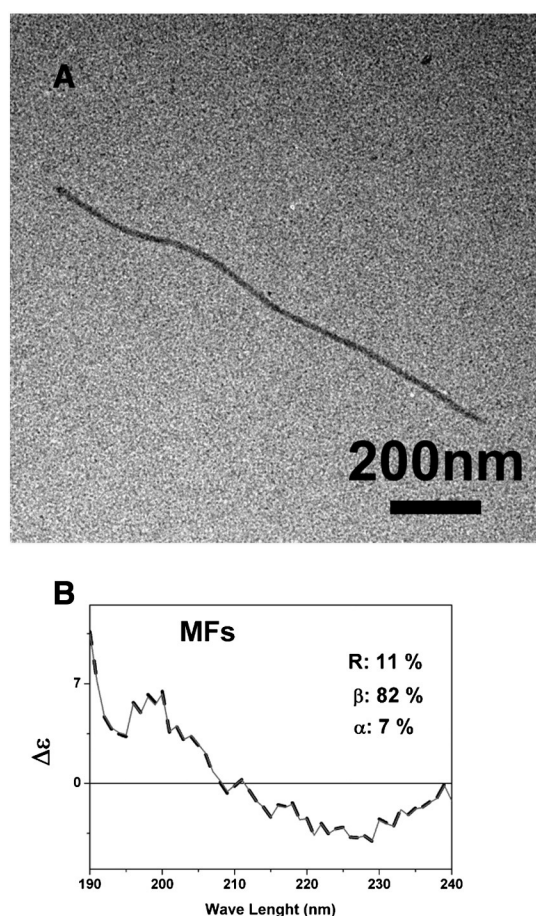


Fig. 6. (A) Representative image of a MF, obtained by negative staining and EF-TEM. The sample was relative to the peak close to the void volume, in the high (160 mM) ionic strength column. (B) CD spectra (full line) together with the numerical fitting (dashed line) and the obtained structure percentages indicate that, as expected, the dominant conformation was the β structure.

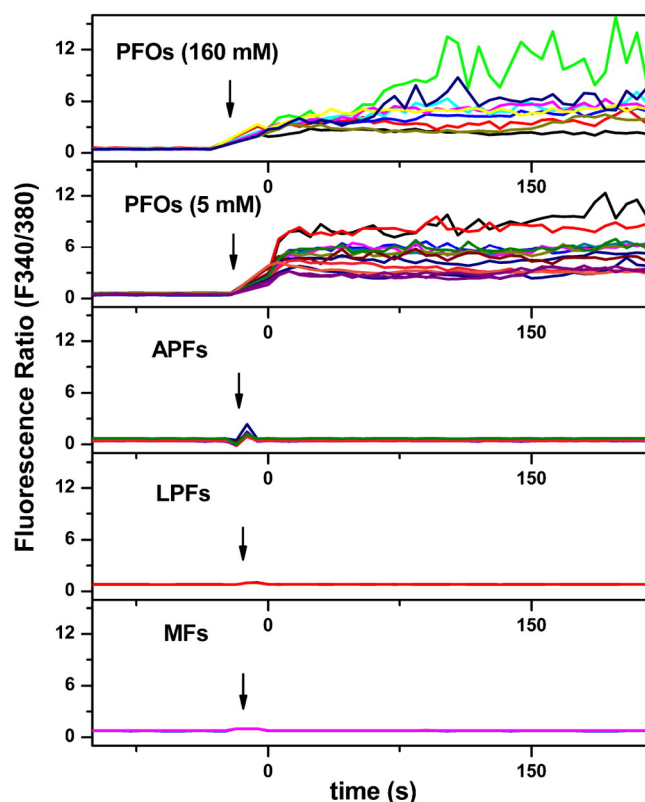


Fig. 7. Ca^{2+} -influx in primary hippocampal neurons, treated with SEC fractions enriched with different sCT aggregates. Optical fluorimetric recordings with Fura-2AM were used to evaluate the intracellular calcium concentration ($[\text{Ca}^{2+}]_i$). sCT fractions were given directly to the wells on the microscope stage, after 10 min recording. Only populations enriched with PFOs, at all ionic strength, were able to instantly increase the Ca^{2+} -influx.

of PFO-enriched populations, we were able to induce biological effects comparable to those induced by unfractionated samples at the concentration of 80 μM in our previous work. Finally, we note that, evaluating the concentration of the active species in number and not in weight, a smaller concentration for trimers and tetramers (1/3 and 1/4, respectively) would be required to obtain a neurotoxic effect.

observed. In particular, APFs (Fig. 1D), LPFs (Fig. 1C) and MFs (Fig. 1A) induced no effect, as in the case of unfractionated and non-incubated sCT in water.

Neurotoxicity experiments were performed with sCT SEC fractions characterized as before, and results are reported in Fig. 8. We observed biological effects only in the case of neurons treated with samples rich in metastable PFOs.

This result is in good agreement with the well-established concept that fibers and protofibrils, even when characterized by different non-random configurations, are not biologically active. This is also in agreement with Kaye's more recent results [12] describing the neurotoxicity of PFOs versus the ineffective biological action of βA APFs.

Finally, we note that in our experiments many stable monomers and few dimers occurring in water were not able to induce any neurotoxicity.

The effects induced by samples rich in PFOs were small but statistically meaningful, likely due to the coexistence of metastable neurotoxic PFOs and inactive monomers. The sCT aggregates that induced a rapid Ca^{2+} -influx in hippocampal neurons were also able to increase apoptosis at 24 h. It should be highlighted, in this regard, that, although apoptosis was recorded after 24 h, PFO exposure lasted only 20 min.

We hypothesize that the brief treatment with PFOs, inducing a rapid Ca^{2+} influx, triggers the apoptotic pathway, supporting the "amyloid-channel" hypothesis, which suggests that neurotoxicity is induced by the permeabilization of the neuronal membrane [33] by metastable PFOs. It is worth emphasizing that, using concentrations of about 8 μM

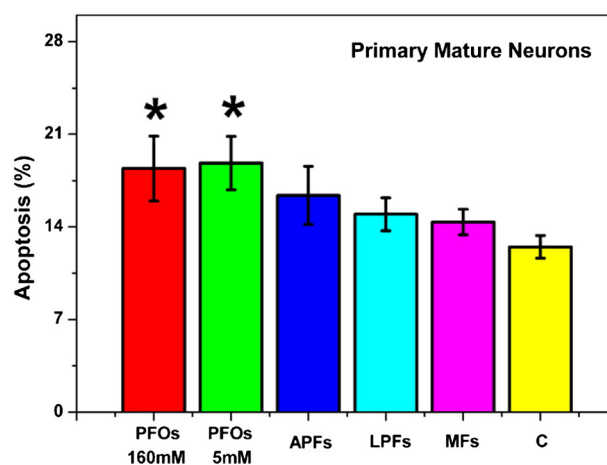


Fig. 8. Neurotoxicity results relative to the studied SEC fractions enriched with different sCT aggregates in primary mature hippocampal neurons. Only populations enriched in PFOs, at all ionic strengths, were biologically active. Apoptosis was measured as percentage of total cells. The bars represent means \pm SEM from four different experiments in duplicate. * $p < 0.05$ with respect to the control.

4. Conclusions

Our data strongly suggest that native and metastable sCT PFOs, composed of dimers, trimers and tetramers, are the only neurotoxic species among the various amyloid sCT aggregates formed in saline solution as final off-pathway products, independently derived from monomeric sCT [6]. In fact, samples containing these metastable structures, even as a minority, were able to induce strong Ca^{2+} influx and apoptosis in mature primary neurons. Conversely, samples mainly made of stable monomers, as in non-incubated and unfractionated sCT in water, were totally ineffective (under the statistical test sensitivity).

Metastable sCT PFOs are very similar to oligomers described in literature for several other amyloid proteins, disease-related or not. In particular, Ono et al. determined the degree of toxicity of dimers, trimers and tetramers of βA , showing that they were 3-, 8- and 13-fold more toxic than the monomer. Furthermore, in the same paper, Ono et al. reported electron microscopy and CD results relative to pure populations of βA oligomers. They showed that trimers and tetramers were around 10 nm in diameter, while monomers and dimers were around 1.5 nm and that the majority of the protein conformation (more than 55%) was RC even in the tetrameric aggregate [16]. Noticeably, all Ono's results were obtained after PICUP treatment to stabilize the protein aggregation.

Our results on the neurotoxicity of sCT, another amyloid protein and obtained without PICUP, can be well interpreted on the basis of the toxicity mechanisms hypothesized for βA aggregates. This observation strongly supports the hypothesis of a common neurotoxicity mechanism for the amyloid proteins [33]. Moreover, our images of globules of about 9 nm diameter can be considered as the direct visualization of native, toxic and metastable trimers and tetramers. For what concerns the protein conformation, the coexistence in our populations of the toxic PFOs with biologically inactive monomers can well explain the more evident RC conformation.

We established that sCT, in our incubation conditions, was unable to create other biologically active, low-molecular-weight aggregates like pentamers and so on. A small number of native, metastable PFOs of low molecular weight was sufficient to render the sample neurotoxic and the early assembly of sCT in APFs or LPFs completely inhibited the biological effects induced on mature neurons through a membrane permeabilization mechanism that could be common to the amyloid family [33].

As for the morphological and structural characterization of the amyloid active aggregate, our results can address further studies in-silico, in synthetic systems, in-vitro and in-vivo to design new therapeutic strategies or to discourage a possibly dangerous therapeutic use of such molecules [34].

Acknowledgments

The authors wish to thank Monica Brocco for the helpful revision of English. This work was supported by the research funds (cap. 524) of the Italian "Istituto Superiore di Sanità".

Appendix A. Supplementary data

Supplementary data to this article can be found online at <http://dx.doi.org/10.1016/j.bbdis.2014.06.006>.

References

- [1] C.A. Ross, M.A. Poirier, Protein aggregation and neurodegenerative disease, *Nat. Med.* 10 (2004) S10–S17.
- [2] B.L. Kagan, R. Azimov, R. Azimova, Amyloid peptide channels, *J. Membr. Biol.* 202 (2004) 1–10.
- [3] M.M. Apetri, N.C. Maiti, M.G. Zagorski, P.R. Carey, V.E. Anderson, Secondary structure of alpha-synuclein oligomers: characterization by Raman and atomic force microscopy, *J. Mol. Biol.* 355 (2006) 63–71.
- [4] M.A. Poirier, H. Li, J. Macosko, S. Cai, M. Amzel, C.A. Ross, Huntingtin spheroids and protofibrils as precursors in polyglutamine fibrilization, *J. Biol. Chem.* 277 (2002) 41032–41037.
- [5] C.M. Dobson, Protein folding and misfolding, *Nature* 426 (2003) 884–890.
- [6] A. Jan, D.M. Hartley, H.A. Lashuel, Preparation and characterization of toxic A β aggregates for structural and functional studies in Alzheimer's disease research, *Nat. Protoc.* 5 (6) (2010) 1186–1209.
- [7] K. Broersen, F. Rousseau, J. Schymkowitz, The culprit behind amyloid-beta peptide related neurotoxicity in Alzheimer's disease: oligomer size or conformation? *Alzheimers Res. Ther.* 2 (4) (2010) 12–14.
- [8] M. Stefani, Biochemical and biophysical features of both oligomer/fibril and cell membrane in amyloid cytotoxicity, *FEBS J.* 277 (2010) 4602–4613.
- [9] M. Bucciantini, E. Giannoni, F. Chiti, F. Baroni, L. Formigli, J. Zurdo, N. Taddei, G. Ramponi, C.M. Dobson, M. Stefani, Inherent toxicity of aggregates implies a common mechanism for protein misfolding diseases, *Nature* 416 (2002) 507–511.
- [10] H.A. Lashuel, P.T. Lansbury Jr., Are amyloid diseases caused by protein aggregates that mimic bacterial pore-forming toxins? *Q. Rev. Biophys.* 39 (2006) 167–201.
- [11] R. Kaye, E. Head, J.L. Thompson, T.M. McIntire, S.C. Milton, C.W. Cotman, C.G. Glabe, Common structure of soluble amyloid oligomers implies common mechanism of pathogenesis, *Science* 300 (2003) 486–489.
- [12] R. Kaye, A. Pensalfini, L. Margol, Y. Sokolov, F. Sarsoza, E. Head, J. Hall, C. Glabe, Annular protofibrils are a structurally and functionally distinct type of amyloid oligomer, *J. Biol. Chem.* 284 (2009) 4230–4237.
- [13] R. Roychoudhuri, M. Yang, M.M. Hoshi, D.B. Teplow, Amyloid beta-protein assembly and Alzheimer disease, *J. Biol. Chem.* 284 (2009) 4749–4753.
- [14] D.B. Teplow, Preparation of amyloid beta-protein for structural and functional studies, *Methods Enzymol.* 413 (2006) 20–33.
- [15] G. Bitan, D.B. Teplow, Rapid photochemical cross-linking: a new tool for studies of metastable, amyloidogenic protein assemblies, *Acc. Chem. Res.* 37 (6) (2004) 357–364.
- [16] K. Ono, M.M. Condron, D.B. Teplow, Structure–neurotoxicity relationships of amyloid beta-protein oligomers, *Proc. Natl. Acad. Sci. U. S. A.* 106 (2009) 14745–14750.
- [17] M. Diociaiuti, M.C. Gaudiano, F. Malchiodi-Albedi, The slowly aggregating salmon Calcitonin: a useful tool for the study of the amyloid oligomers structure and activity, *Int. J. Mol. Sci.* 12 (2011) 9277–9295.
- [18] M. Diociaiuti, L. Zanetti Polzi, L. Valvo, F. Malchiodi-Albedi, C. Bombelli, M.C. Gaudiano, Calcitonin forms oligomeric pore-like structures in lipid membranes, *Biophys. J.* 91 (2006) 2275–2281.
- [19] F. Malchiodi-Albedi, V. Contrucci, C. Raggi, K. Fecchi, G. Rainaldi, S. Paradisi, A. Matteucci, M.T. Santini, M. Sargiacomo, C. Frank, M.C. Gaudiano, M. Diociaiuti, Lipid raft disruption protects mature neurons against amyloid oligomer toxicity, *Biochim. Biophys. Acta* 1802 (2010) 406–415.
- [20] D. Hall, L. Huang, On the use of size exclusion chromatography for the resolution of mixed amyloid aggregate distributions: I. Equilibrium partition models, *Anal. Biochem.* 426 (1) (2012) 69–85.
- [21] J. Wen, T. Arakawa, J.S. Philo, Size-exclusion chromatography with on-line light-scattering, absorbance, and refractive index detectors for studying proteins and their interactions, *Anal. Biochem.* 240 (1996) 155–166.
- [22] F. Malchiodi-Albedi, S. Paradisi, A. Matteucci, C. Frank, M. Diociaiuti, Amyloid oligomer neurotoxicity, calcium dysregulation, and lipid rafts, *Int. J. Alzheimers Dis.* (2011), <http://dx.doi.org/10.4061/2011/906964> (Article ID 906964, 17 pages).
- [23] M.D. Ledesma, B. Brugger, C. Bunning, F.T. Wieland, C.G. Dotti, Maturation of the axonal plasma membrane requires upregulation of sphingomyelin synthesis and formation of protein–lipid complexes, *EMBO J.* 18 (1999) 1761–1771.
- [24] S.S. Wang, T.A. Good, D.L. Rymer, The influence of phospholipid membranes on bovine calcitonin secondary structure and amyloid formation, *Protein Sci.* 14 (2005) 1419–1428.
- [25] F. Rahimi, P. Maiti, G. Bitan, Photo-induced cross-linking of unmodified proteins (PICUP) applied to amyloidogenic peptides, *J. Vis. Exp.* (23) (2009 Jan 12) (pii: 1071).
- [26] M. Diociaiuti, Electron energy loss spectroscopy microanalysis and imaging in the transmission electron microscope: example of biological applications, *J. Electron Spectrosc. Relat. Phenom.* 143 (2006) 189–203.
- [27] L. Whitmore, B.A. Wallace, Protein secondary structure analyses from circular dichroism spectroscopy: methods and reference databases, *Biopolymers* 89 (2008) 392–400.
- [28] L. Whitmore, B.A. Wallace, DICHROWEB, an online server for protein secondary structure analyses from circular dichroism spectroscopic data, *Nucleic Acids Res.* 32 (2004) W668–W673.
- [29] G.J. Brewer, J.R. Torricelli, E.K. Evege, P.J. Price, Optimized survival of hippocampal neurons in B27-supplemented Neurobasal, a new serum-free medium combination, *J. Neurosci. Res.* 35 (1993) 567–576.
- [30] F. Malchiodi-Albedi, M.R. Domenici, S. Paradisi, A. Bernardo, M.A. Ajmone-Cat, L. Minghetti, Astrocytes contribute to neuronal impairment in beta A toxicity increasing apoptosis in rat hippocampal neurons, *Glia* 34 (2001) 68–72.
- [31] C. Frank, A.M. Giammaroli, R. Pepponi, S. Fiorentini, S. Rufini, Cholesterol perturbing agents inhibit NMDA-dependent calcium influx in rat hippocampal primary culture, *FEBS Lett.* 566 (2004) 25–29.
- [32] H.A. Lashuel, D. Hartley, B.M. Petre, T. Walz, P.T. Lansbury Jr., Neurodegenerative disease: amyloid pores from pathogenic mutations, *Nature* 418 (2002) 291.
- [33] C.G. Glabe, Common mechanisms of amyloid oligomer pathogenesis in degenerative disease, *Neurobiol. Aging* 27 (2006) 570–575.
- [34] F. Malchiodi-Albedi, N. Vanacore, M. Diociaiuti, Calcitonin therapy and oligomer neurotoxicity: an underestimated risk? *Neurotoxicology* 29 (2008) 1150–1151.